Available online at www.sciencedirect.com
SCIENCE DIRECT®
International Journal of Mass Spectrometry 230 (2003) 175–183
International Journal of Mass Spectrometry
www.elsevier.com/locate/ijms

The kinetic method reveals secondary deuterium isotope effects on the proton affinity and gas-phase basicity of glycine and alanine methyl esters

S.P. Mirza [a], P. Krishna [a], S. Prabhakar [a], M. Vairamani [a], D. Giblin [b], Michael L. Gross [b,*]

[a] *Indian Institute of Chemical Technology, Hyderabad 500 007, India*
[b] *Department of Chemistry, Mass Spectrometry Research Resource, Washington University, St. Louis, MO 63130, USA*

Received 28 July 2003; accepted 21 August 2003

Abstract

The kinetic method for measuring proton affinities (PA) and gas-phase basicities (GB) was applied to the methyl esters of simple amino acids. The experiments show that the GB and PA values for deuterium labeled glycine methyl ester are indeed greater than that of the corresponding unlabelled glycine methyl ester. The PA of L-Ala-OCD_3 is also slightly greater than that of the unlabeled alanine methyl ester. The secondary isotope effects originate, as shown by density functional theory, in differences in zero-point energies and thermal-energy corrections between H and D-bearing molecules.

Keywords: Secondary deuterium isotope effect; Proton affinity; Glycine; Density functional theory

1. Introduction

Labelling studies have long been used to probe structure and mechanism in both solution and gas-phase chemistry. In particular, deuterium labelling studies have been widely used in the study of reaction mechanisms, and have provided a wealth of information towards elucidating and verifying the structure of reactive intermediates and affording details of isomerization in liquid and gas phases [1]. Recently, isotopic labelling has moved into proteomic applications with the introduction of the isotope-coded affinity tag reagent in quantitative proteomics [2]. Labelling studies are also being widely used in the chiral recognition mass spectrometry [3,4].

Isotopic labelling can lead to a primary, large kinetic isotope effect when the labelled atom is involved in the rate-determining step. Secondary kinetic isotope effects are small because the labelled atom is not directly involved in the bond breaking/forming process. In addition, small isotope effects are also observed in the near-threshold ionisation of labelled molecules and also in equilibrium reactions involving ions and neutrals with labelled analogs [5,6].

Although small isotope effects are difficult to measure accurately, the kinetic method is appropriate for this task. We report here the measurement of small secondary isotope effects in the metastable-ion decomposition of proton-bound adducts of methyl esters of amino acids and their d_3-methyl analogs. In this study, we measured the difference in gas-phase basicities of several amino acid methyl esters (alanine, β-alanine, and glycine) and the corresponding d_3-methyl analogs by using the kinetic method. In addition, we augmented the experimental work with calculations of the difference in the gas-phase basicity of methyl glycinate and its d_3-analog by using density functional theory (DFT).

We are pleased to dedicate this article to John Beynon on the occasion of his 80th birthday. Professor Beynon is the pioneering figure in tandem mass spectrometry, starting with mass analysed ion kinetic energy spectrometry, a key technique in this investigation.

2. Experimental

The methyl esters of certain amino acids, L-alanine, L-phenylalanine, L-phenylglycine and L-leucine, in addition to those of glycine and β-alanine, and their deuterated (d_3-methyl) analogs [4] were synthesized by using standard procedures [7].

* Corresponding author. Tel.: +1-314-935-4814; fax: +1-314-935-7484.
E-mail address: mgross@wuchem.wustl.edu (M.L. Gross).

1387-3806/$ – see front matter © 2003 Elsevier B.V. All rights reserved.
doi:10.1016/j.ijms.2003.08.009

2.1. Mass spectrometry

ESI mass spectra and mass analysed ion kinetic energy (MIKE) product-ion spectra were acquired by using the Indian Institute of Chemical Technology Autospec M (Micromass, Manchester, UK) mass spectrometer interfaced with an OPUS V3.IX data system. The samples were dissolved in glycerol or 3-nitrobenzyl alcohol matrices and were ionized by a primary beam of cesium ions of 25-keV energy. The ion-source temperature was 45 °C. The desorbed ions were accelerated to 8 kV. Normal mass spectra and MIKE experiments were carried out with the same instrument. The precursor ion of interest was selected by using the first electric and magnetic sectors, decompositions were allowed to take place in the field-free region between the magnetic and second electrostatic analyser, and the spectra of the product ions were obtained by scanning the second electrostatic analyser.

Electrospray (ESI) ionization experiments were conducted by using a Thermo Finnigan LCQ quadrupole ion-trap mass spectrometer at Washington University. The spray voltage was 4.2 kV, and the capillary temperature was in the range of 150–200 °C. For bracketing measurements, the methyl esters of the amino acids (100-μM solutions in 50% methanol and water) were mixed with equimolar amounts of the reference compounds before the analysis. The mixture was introduced into the ESI source with a syringe pump at a flow of 5 μl/min. MS/MS experiments were done by selecting the ion of interest with an isolation width of 4 *m/z* units. Ten scans in a single run were summed, and three such sets were taken at each selected collision energy and averaged for the calculations. In this instrument, the MS/MS experiments are low-energy and involve numerous collisions with the He buffer gas.

A sample mixture containing equimolar amounts of an amino acid methyl ester and its d_3-methyl analogue were dissolved either in a glycerol matrix for LSIMS or in the 50% methanol in water solution for ESIMS. The procedure allowed us to optimize the formation of the target proton-bound hetero dimer relative to the production of the proton-bound homo dimers. In addition, protonated monomers were formed.

2.2. Theoretical calculations

The goal of the theoretical calculations was to account for the secondary isotope effects in terms of the gas-phase proton affinities of the selected methyl and d_3-methyl amino acids. For calculation efficiency, only the methyl ester of glycine was investigated. Structural optimization of the neutral and protonated form began by scanning conformation space using Monte Carlo simulations as available in Spartan [8] (v. 02 for Linux). Each form of the ion or neutral was "heated" to 5000 K and then annealed at 300 K. All resulting distinct structures were subjected to optimization by the PM3 semi-empirical algorithm [9] and verified as minima by vibrational-frequency analysis.

All subsequent calculations were performed by using the Gaussian 98 [10] suite of programs (v. A.7). Methods of density functional theory (DFT) were chosen because they perform well in geometric optimizations and energy calculations [11], requiring less computational overhead than do the traditional perturbation methods. Structural optimizations and frequency calculations on the stable isomers of neutral and singly-protonated methyl glycinate were ultimately carried out with the hybrid B3LYP functional in conjunction with the basis set, 6-311+G(2d,p), as available in Gaussian 98 [10]. All optimized structures were verified to exist at local minima by vibrational-frequency analysis with analytical second derivatives. Secondary isotope effects are manifest in the zero-point vibrational energies (ZPE) and thermal-energy corrections, both of which are based on vibrational-frequency fundamentals. (Isotopic substitution changes the vibrational frequencies through resultant differences in mass but does not affect geometry or vibrational force constants.) To enhance relative accuracy of the important lower frequency contributions, the geometric optimizations were performed with Tight cutoffs on forces and step size, and the numerical integration step in DFT used the UltraFine grid (99,590, pruned) [10]. Zero-point vibrational energies (ZPE) were scaled by 0.9806, and the vibrational fundamentals by 1.0013 [12]. These scaling factors were optimized for lower-frequency contributions to the thermal-energy corrections. In addition, the most stable conformer of both neutral and protonated methyl glycinate was subjected to geometric optimization and vibrational frequency determination at the level QCISD/6-31G(d). In this case, the scaling factors were 0.9776 and 1.0147 for the ZPE and vibrational frequencies [12], respectively.

3. Results and discussion

The mass analysed ion kinetic energy (MIKE) spectrum of the proton-bound hetero dimer of L-methyl alaninate (L-Ala-OCH_3) and L-d_3-methyl alaninate (L-Ala-OCD_3), [L-Ala-OCH_3 + L-Ala-OCD_3 + H]$^+$ showed as products the protonated monomers of both L-Ala-OCH_3 and L-Ala-OCD_3. The [L-Ala-OCD_3 + H]$^+$ was produced more abundantly than [L-Ala-OCH_3 + H]$^+$, indicating the higher gas-phase basicity (GB) of L-Ala-OCD_3 relative to L-Ala-OCH_3 (Fig. 1a). When this set of experiments was carried out with D-methyl alaninate and its corresponding d_3-labelled compound, identical results were produced. This reveals that the observed difference is due to labelling and not due to any latent chirality effect. Furthermore, the same set of competitive MIKE experiments were carried out with β-methyl alaninate (Fig. 1b), methyl glycinate (Fig. 1c), and methyl *p*-aminobenzoate in the presence of the corresponding d_3-analogs in all cases produced similar results wherein the more abundant product ion was the d_3-labelled analogue. This interesting observation prompted

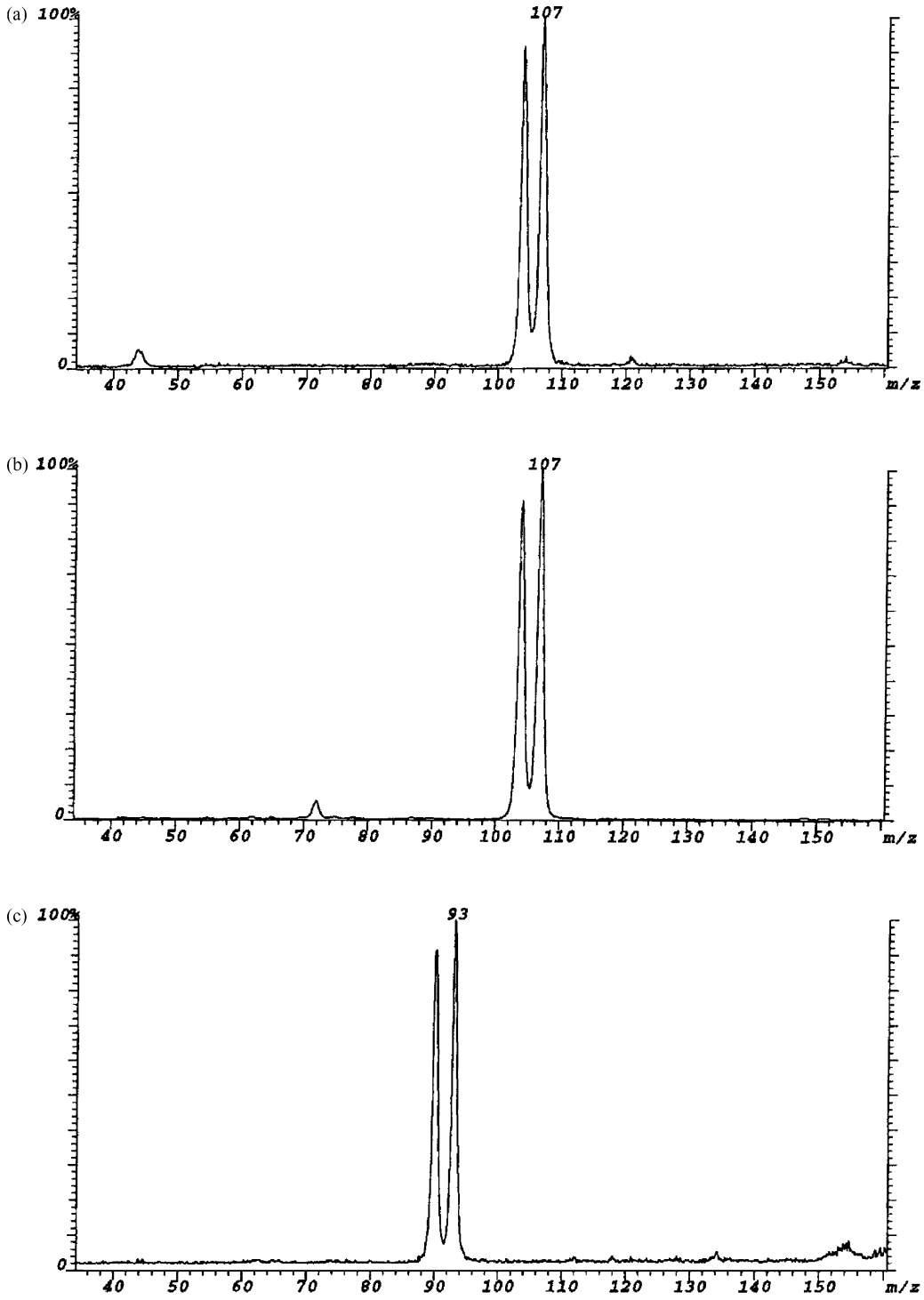

Fig. 1. MIKE spectrum of proton-bound hetero dimer of (a) L-Ala-OCH_3 and L-Ala-OCD_3, (b) β-Ala-OCH_3 and β-Ala-OCD_3, (c) GlyOCH_3 and GlyOCD_3.

us to undertake a more detailed investigation to estimate the GB values of selected amino acid methyl esters and their deuterated analogues, which are not available in the literature.

We employed the kinetic method [13] to estimate the GB value, because the kinetic method is sufficiently sensitive to measure the expected small difference in GB between L-Ala-OCH_3 and L-Ala-OCD_3. By using the kinetic method, the GB of an unknown is calculated from the rates of competitive dissociation of mass-selected hetero-cluster ions containing both the unknown and a known reference compound. For example, the proton-bound dimer, $A\cdots H^+\cdots B$, dis-

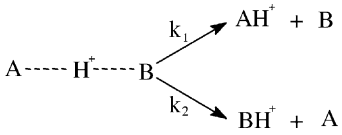

Scheme 1.

sociates as shown in Scheme 1, where the k_1 and k_2 are the rate constants for the competitive dissociation reactions; the rate constants are reflected by the appropriate product-ion abundances [14]:

$$\ln\frac{[AH^+]}{[BH^+]} = \frac{GB(A) - GB(B)}{RT_{eff}} \quad (1)$$

The kinetic method has its basis in transition-state theory and assumes that the measured abundances reflect rate constants, that there are no reverse activation barriers, and that the partition functions of the transition states of the two dissociation channels are virtually identical (Eq. (1)). A plot of the natural logarithm of the abundance ratio of protonated monomer ions, AH^+ (considered the analyte) and BH^+ (considered the referent), $\ln([AH^+]/[BH^+])$, versus the GB of a series of similar, and bracketing, reference compounds gives a linear relationship that can be used to determine the unknown GB(A). Specifically, the unknown GB(A) is derived from the intercept where $\ln([AH^+]/[BH^+]) = 0$, hence $GB(A) = GB_{int}$; the effective temperature, T_{eff}, is derived from the slope. Although the validity of the kinetic method as a general method has been questioned, its simplicity and its compatibility with non-volatile molecules in an equilibrium measurement have lead to its wide use [14]. In addition, its applicability has been extended to cases where the GB of the analytes differed only slightly [15]. Several modifications have also been proposed for improving the values obtained by the kinetic method [16–20].

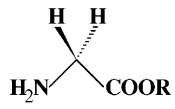

R = CH_3 ; $GlyOCH_3$
CD_3 ; $GlyOCD_3$

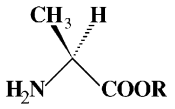

R = CH_3 ; L-$AlaOCH_3$
CD_3 ; L-$AlaOCD_3$

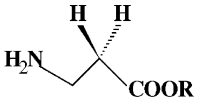

R = CH_3 ; β-$AlaOCH_3$
CD_3 ; β-$AlaOCD_3$

In the present study, we measured the GB values of L-Ala-OCH_3, L-Ala-OCD_3, β-Ala-OCH_3, β-Ala-OCD_3, Gly-OCH_3, and Gly-OCD_3 by the simple kinetic method (Table 1). We chose as reference compounds amino acids because they are closely related in structure; we carefully selected the reference amino acids so that the GB values of the references would be close and bracketing to those of the amino acid methyl esters of interest. We could not find more than two amino acids as references for methyl glycinate, however, and hence, we selected halo-pyridines as references for these compounds. We also could not locate more than three references among the halo pyridines. 3-Fluoropyridine does fall within the expected gas-phase basicity range; the MS/MS decomposition of the proton-bound hetero dimer gives significant additional peaks during fragmentation even at low collision energy. For L-Ala-OCH_3 and L-Ala-OCD_3, we used L-phenylalanine, L-leucine, L-isoleucine and L-valine as reference compounds and for β-Ala-OCH_3 and β-Ala-OCD_3, L-phenylalanine, L-aspargine, L-proline, L-methionine and L-tryptophan are used as reference amino acids. For the glycine esters, we used 2-bromopyridine, 2-chloropyridine, and 3-chloropyridine. The GB values of reference amino acids and halo-pyridines used in the estimation of GB values are taken from the work of Harrison [21] or the compilation of Hunter and Lias [22].

The data for the first round of the kinetic-method experiments came from MIKES experiments. We found, however, that the correlation coefficients obtained from the plots of the MIKES data for the amino-acid methyl esters versus GB of the corresponding standards depended strongly on the reference scale used, and, more importantly, the correlation coefficients were not satisfactory. The dependence upon reference scale may point to inaccuracies in the available gas-phase basicity or proton affinity values for the amino acids.

We then turned to the quadrupole ion-trap instrument for generating the data for proton-bound materials that were introduced by electrospray ionization. We used MS/MS experiments at a series of collision energies ranging from 18 to 30% of the maximum available collision energy (5 eV, laboratory frame of reference) to dissociate the proton-bound materials. We selected the collision energy range 18–30% of 5 V in the ion trap because below 18% the decomposition of the dimer ion is not significant whereas above 30%, additional fragmentation starts. However, we found essentially no variation or trend in either the GB values or T_{eff} obtained as a function of the collision energy in the 18–30% range. Hence, we could not apply the modified kinetic method for this work and, instead, we used the simple kinetic method and averaged the GB and T_{eff} values taken at various collision energies (Table 1).

The correlation coefficients obtained for the alanine esters varies from 0.92 to 0.93; for β-alanine esters they are in the range of 0.98–0.99, and for glycine esters, in the range of 0.98–0.99. For those systems giving poorer correlations, uncertainty in the literature GB values for the amino acids used as references may be responsible.

Are the experimental differences in the GB values (Table 1) significant? Employing the standard *t*-test for comparison of averages, we may conclude that indeed the GB of Gly-OCD_3 is greater than that of the unlabeled glycine methyl ester at the 95% confidence level, whereas the GB of Ala-OCD_3 is greater than the unlabeled compound at the confidence level. The difference in GB values for β-alanine methyl ester, however, cannot be distinguished even at 75% confidence.

When we used the proton-affinity values for amino acids that were reported by Bojensen and Breindahl [23], we

Table 1
Gas-phase basicity (GB) values (kcal/mol) of the amino acid methyl esters determined by the kinetic method

Collision energy percentage of 5 eV	L-Ala-OCH_3	L-Ala-OCD_3	β-Ala-OCH_3	β-Ala-OCD_3	Gly-OCH_3	Gly-OCD_3
18	209.7	209.8	214.45	214.40	207.67	207.68
20	209.6	209.7	214.36	214.37	207.67	207.77
25	209.6	209.6	214.30	214.30	207.69	207.75
28	209.6	209.6	214.29	214.30	207.70	207.76
30	209.6	209.7	214.29	214.30	207.68	207.70
Average	209.6	209.7	214.34	214.33	207.68	207.73
S.D.	0.1	0.1	0.07	0.05	0.01	0.04
[a] t	1.6		0.3		3.2	
[b] T_{eff} (avg) (K)	399		335		283	

[a] The t-values were calculated for comparison of averages. For eight degrees of freedom (10 total determinations), the critical t-value are 2.3, 1.9, and 1.4 for 95, 90 and 75% confidence levels, respectively. An experimental value of 't' that is greater indicates a significant difference for that confidence level.
[b] T_{eff} (avg) are the effective temperatures averaged over all the measurements for each methyl ester and its d_3-analog. There were no trends noted in the small changes in T_{eff} for each methyl ester.

obtained better correlations for all our experimental data (Table 2). The use of proton affinity values in place of gas-phase basicity values provides relative enthalpies instead of free energies [14,20]. For proton affinities, we may conclude, after comparing averages using the t-test, that L-Ala-OCD_3 has a greater GB than does L-Ala-OCH_3 at 95% confidence level. The difference for β-Ala-OCD_3 and β-Ala-OCH_3 is smaller and not significant even at 75% confidence (Table 2).

Others studied, using the kinetic method, the effects of deuterium substitution on proton affinity (PA) and gas-phase acidity (GA) for a variety of other compounds [24,25]. For example, the gas-phase basicity of α-deuterium labeled ethanol is lower than that of unlabeled ethanol [14]. When the position of labelling is changed from the α to the β-carbon in ethanol, the difference in the GA between ethanol and its β-deuterated analogue decreased. The authors concluded that β-deuteration induces no measurable isotope effect. Deuterium labelling in L-Ala-OCD_3 at the δ-position relative to the site of protonation, however, does produce a small but significant difference in the PA values of the unlabeled and deuterated analog (Table 2), but no other pair wise comparisons can be made of the GB or PA values for the two alanine esters because the precision is insufficient to permit such.

3.1. Theory

To account for the small, experimental differences in the GB values of the unlabeled and d_3- methyl esters, we looked for a theoretical justification for the differences manifest in the decompositions of the proton-bound dimers. Using the assumptions of the kinetic method, we made use of the competition for the proton between the unlabeled and d_3-methyl esters in the decomposition of the proton-bound heterodimer that reflects the position of equilibrium in the proton-transfer reaction:

$$(M + H)^+ + d_3{-}M \rightleftarrows M + (d_3{-}M + H)^+ \quad (2)$$

where 'M' and 'd_3-M' refer to the methyl and d_3-methyl esters of glycine, respectively. For this reaction, there is no net $\Delta(PV)$ work, and (ΔS) is virtually zero. Hence, the energy of reaction, ΔE_r, becomes the same as the enthalpy of reaction, $\Delta H_r = PA(M) - PA(d_3{-}M)$, and the free energy of reaction, $\Delta G_r = GB(M) - GB(d_3{-}M)$. We used density functional theory, as described in the previous section, to do the calculations. Previous ab initio studies of the methyl

Table 2
Gas-phase PA values (kcal/mol) of the amino acid methyl esters determined by the kinetic method

Collision energy percentage of 5 eV	L-Ala-OCH_3	L-Ala-OCD_3	β-Ala-OCH_3	β-Ala-OCD_3
18	218.56	218.59	222.20	222.23
20	218.52	218.59	222.14	222.16
25	218.50	218.57	222.09	222.12
28	218.52	218.57	222.07	222.08
30	218.48	218.54	222.02	222.06
Average	218.51	218.57	222.10	222.13
S.D.	0.03	0.02	0.06	0.06
[a] t	2.6		0.9	

[a] The t-values were calculated for comparison of averages. For 8 degrees of freedom (10 total determinations), the critical t-value are 2.3, 1.9, and 1.4 for 95, 90 and 75% confidence levels, respectively. An experimental value of 't' that is greater indicates a significant difference for that confidence level.

Table 3
Calculated energies of neutral and protonated methyl and d_3-methyl esters of glycine

Isomer[a]	Electronic energy (hartree)	Normal		Deuterated-d_3		ΔE (kcal/mol)
		Thermal correction (kcal/mol)[b]	Relative energy (kcal/mol)	Thermal correction[b] (kcal/mol)	Relative energy (kcal/mol)	
Level: B3LYP/6-311+G(2d,p)						
N1	−324.203649	81.048	0.000	75.007	0.000	6.041
N2	−324.194882	81.250	5.703	75.211	5.706	6.039
N3	−324.188372	80.752	9.290	74.722	9.302	6.030
O1	−324.180913	79.825	13.044	73.775	13.036	6.049
O2	−324.169064	80.107	20.761	74.043	20.738	6.064
O3	−324.164000	79.849	23.681	73.823	23.696	6.026
O4	−324.166372	79.689	22.033	73.635	22.019	6.055
O5	−324.157585	79.927	27.784	73.873	27.772	6.053
I1	−323.847138	71.962	0.000	65.961	0.000	6.001
I2	−323.845212	71.883	1.130	65.879	1.127	6.004
I3	−323.844728	71.974	1.525	65.972	1.523	6.002
I4	−323.843041	71.931	2.540	65.927	2.537	6.003
I5	−323.834986	71.834	7.497	65.830	7.495	6.003
I6	−323.831534	72.017	9.846	65.992	9.823	6.025
					ΔE_r	−0.039
Level: QCISD/6-31G(d)						
N1Q	−323.162658	83.873		77.614		6.259
I1Q	−322.799596	74.382		68.155		6.228
					ΔE_r	−0.031

ΔE: difference in corrected energies between corresponding unlabeled and d_3-methylated isomers. As discussed in Section 2, these differences are entirely the differences in the thermal energy corrections between the unlabeled and d_3-methylated isomers. $\Delta E_r = \Delta H_r = \Delta G_r$: energetics of the proton-transfer reaction (Eq. (2)), calculated using isomers with relative energies < 5.0 kcal/mol of the lowest energy protonated and neutral forms.

[a] There were found three conformers for protonation at the amine N (Nx) and five for protonation at the carbonyl O (Ox). There were no stable forms found for protonation at the ester O. In addition, there were found six conformers for neutral methyl glycinate (Ix).

[b] Thermal correction: $(E_{298} - E_0) + \text{ZPE}$ for standard temperaure (298.15 K) and pressure.

ester of glycine focussed upon geometry as a function of the level of theory and basis set [26] and upon the calculation of the proton affinity for comparison purposes with metal cation binding [27]. To our knowledge, there are no other published calculations of the methyl esters or of the effect of isotope labelling on the proton affinities or other properties of methyl esters of amino acids.

The calculated energies for the stable isomers and conformers of neutral and protonated methyl glycinate are presented in Table 3. The calculated values for $\Delta E_r = \Delta H_r$ of −0.039 (or −0.031) kcal/mol (depending on level) predicts a ∼0.94:1.00 ratio of unlabeled to d_3-methylated product ions abundance. These results compare favorably with $\Delta\text{PA} = -\Delta H_r = 0.05$ kcal/mol from Table 1 and the ratio of ∼0.90:1.00 from Fig. 1c.

The optimized geometries for the most stable conformer of neutral and N- and O-protonated methyl glycinate are presented in Fig. 2, and the bond lengths, angles, and dihedrals for all isomers and conformers are given in Table 4.

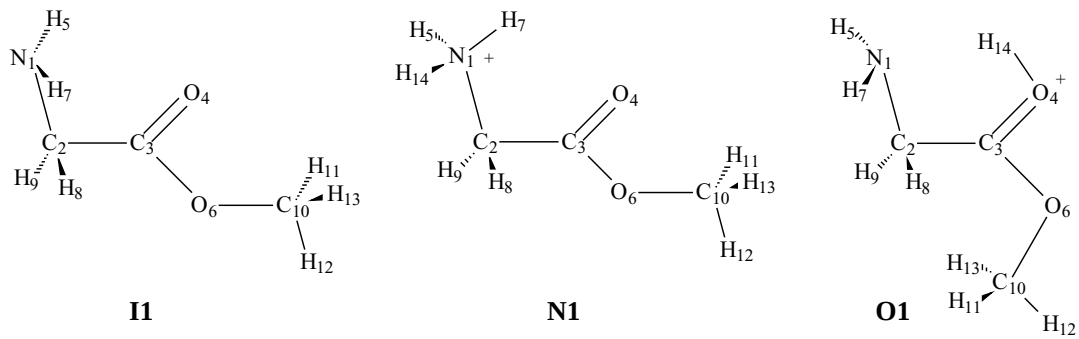

Fig. 2. Geometries of the most stable conformers of neutral and *N*- and *O*(carbonyl)-protonated methyl glycinate. Bond lengths, angles, and dihedrals for all isomers and conformers are given in Table 4.

Table 4
Geometries of the optimized isomers of neutral and protonated methyl glycinate

	Neutral							N-protonated				O-protonated (carbonyl)				
	I1	I1Q	I2	I3	I4	I5	I6	N1	N1Q	N2	N3	O1	O2	O3	O4	O5
Bond lengths (Å)																
N1–C2	1.449	1.456	1.456	1.452	1.461	1.450	1.469	1.508	1.507	1.515	1.505	1.459	1.452	1.453	1.423	1.446
C2–C3	1.525	1.522	1.513	1.527	1.515	1.532	1.527	1.532	1.530	1.527	1.544	1.521	1.509	1.506	1.515	1.516
C3–O4	1.205	1.216	1.206	1.206	1.205	1.201	1.203	1.212	1.220	1.192	1.210	1.267	1.289	1.289	1.284	1.293
C3–O6	1.347	1.352	1.345	1.347	1.347	1.357	1.349	1.303	1.313	1.337	1.307	1.270	1.268	1.273	1.275	1.270
O6–C10	1.440	1.441	1.440	1.440	1.440	1.433	1.437	1.467	1.466	1.466	1.453	1.470	1.484	1.470	1.478	1.470
C2–H8	1.094	1.098	1.102	1.093	1.103	1.094	1.094	1.088	1.093	1.088	1.088	1.093	1.093	1.090	1.098	1.093
C2–H9	1.094	1.098	1.093	1.093	1.090	1.094	1.092	1.088	1.094	1.090	1.088	1.093	1.096	1.090	1.098	1.089
C10–H11	1.090	1.094	1.089	1.089	1.090	1.091	1.092	1.087	1.092	1.087	1.085	1.088	1.087	1.090	1.087	1.087
C10–H12	1.087	1.091	1.087	1.087	1.087	1.087	1.087	1.084	1.089	1.085	1.090	1.084	1.084	1.084	1.084	1.084
C10–H13	1.090	1.094	1.090	1.089	1.089	1.091	1.089	1.087	1.092	1.087	1.090	1.088	1.084	1.090	1.087	1.087
N1–H5	1.015	1.021	1.015	1.014	1.014	1.015	1.015	1.022	1.027	1.024	1.022	1.014	1.014	1.011	1.011	1.011
N1–H7	1.015	1.021	1.013	1.014	1.014	1.015	1.015	1.048	1.042	1.026	1.055	1.014	1.013	1.011	1.011	1.012
N1–H14								1.022	1.028	1.024	1.022	1.736				
O4–H7								1.858	1.975		1.773					
O4–H14												1.025	0.978	0.974	0.978	0.972
Angles																
N1–C2–C3	115.8	114.8	110.4	119.6	113.2	115.0	109.7	105.3	105.8	112.1	104.5	106.4	109.4	102.4	118.2	110.7
C2–C3–O4	125.2	125.0	124.7	123.3	124.3	122.9	121.7	119.8	120.6	121.3	117.7	116.1	116.3	117.3	117.8	121.6
C2–C3–O6	110.9	111.0	111.3	113.0	111.9	118.2	119.2	111.9	111.0	111.2	119.6	126.4	126.8	118.3	125.4	125.9
C3–O6–C10	115.9	114.6	115.7	115.5	115.7	121.2	121.4	117.2	115.9	116.0	122.5	121.9	124.0	122.5	122.5	123.4
C3–C2–H8	107.7	108.1	105.7	106.0	105.6	108.7	105.9	111.2	112.1	110.0	112.0	108.7	107.2	108.9	105.9	108.7
C3–C2–H9	107.7	108.1	108.6	106.0	106.5	108.7	110.3	111.2	110.4	109.3	112.0	108.7	106.4	109.1	105.9	110.1
O6–C10–H11	110.4	110.4	110.3	110.3	110.4	111.6	110.6	109.2	109.3	109.2	104.6	109.4	108.3	109.4	109.0	109.5
O6–C10–H12	105.5	105.2	105.5	105.5	105.5	105.4	105.3	104.6	104.5	105.1	110.6	104.1	103.4	104.4	103.9	103.9
O6–C10–H13	110.4	110.4	110.4	110.3	110.2	111.6	110.9	109.2	109.2	109.1	110.6	109.4	108.1	109.1	109.0	109.3
C2–N1–H5	110.3	108.6	109.7	110.9	110.8	109.8	110.1	113.0	113.3	111.8	113.2	113.2	111.9	113.8	115.0	116.1
C2–N1–H7	110.3	108.6	111.3	110.9	110.2	109.8	110.3	104.0	106.3	109.9	102.8	113.2	111.7	113.9	115.0	116.0
C2–N1–H14								113.0	112.2	111.2	113.2					
C3–O4–H14												102.9	112.7	115.7	112.7	113.2
Dihedrals																
N1–C2–C3–O4	0.0	−0.0	20.6	180.0	−148.0	0.0	105.9	0.0	−8.5	171.2	0.0	0.0	124.9	−86.5	0.0	89.6
N1–C2–C3–O6	180.0	−180.0	−161.2	−0.0	34.8	180.0	−72.9	−180.0	172.4	−9.9	−180.0	180.0	−54.5	89.9	180.0	−84.3
C2–C3–O6–C10	180.0	180.0	−177.0	180.0	178.7	0.0	−2.8	−180.0	178.1	−178.4	0.0	0.0	−3.8	−171.4	0.0	−7.9
O6–C3–C2–H8	56.7	57.1	74.4	−124.2	−91.3	57.3	163.1	60.9	52.4	−130.7	61.4	58.0	178.8	−30.3	55.5	154.7
O6–C3–C2–H9	−56.7	−57.1	−39.5	124.2	155.2	−57.3	46.4	−60.9	−69.5	109.6	−61.4	−58.0	64.5	−149.5	−55.5	37.7
C3–O6–C10–H11	−60.4	−60.4	−60.6	−60.3	−60.7	−61.7	−70.4	−60.6	−60.3	−59.9	−180.0	−61.7	−60.5	−62.9	−61.5	−57.7
C3–O6–C10–H12	180.0	180.0	179.8	−180.0	179.6	180.0	172.0	−180.0	−179.7	−179.5	62.2	180.0	−178.5	179.1	180.0	−176.1
C3–O6–C10–H13	60.4	60.4	60.2	60.3	60.1	61.7	52.8	60.6	60.9	60.9	−62.2	61.7	61.3	61.2	61.5	65.7
C3–C2–N1–H5	58.3	56.7	−34.9	59.0	−58.2	57.7	−65.1	118.4	137.8	170.2	118.2	−118.0	−88.8	−117.2	−65.1	71.6
C3–C2–N1–H7	−58.3	−56.7	−154.9	−59.0	−177.3	−57.7	177.1	−0.0	17.0	48.8	0.0	118.0	149.7	114.4	65.1	−62.0
C3–C2–N1–H14								−118.4	−99.9	−68.8	−118.2					
C2–C3–O4–H14												0.0	179.1	171.3	180.0	8.3

4. Conclusion

The results of the calculated differences in heats of formation are consistent with the experimental results presented here. Both show that the GB and PA values for deuterium labelled glycine methyl ester are indeed greater than those of the corresponding unlabeled glycine methyl ester. The PA of L-Ala-OCD_3 is also slightly greater than that of the unlabeled alanine methyl ester. The secondary isotope effects originate, as shown by density functional theory, in differences in zero-point energies and thermal-energy corrections between H and D bearing molecules.

Others have studied secondary isotope effects on the proton affinities of small molecules in the gas phase. Perhaps the first example is that by Gronert and Williams [28], who used the kinetic method and found that for gas-phase glycine, the PA of H_2NCD_2COOH is greater than that of unlabeled glycine, an inverse effect that is similar to the outcome of our work. Norrman and McMahon [29] reported that the proton affinities of methanol, dimethyl ether, and acetone show normal isotope effects whereas CD_3CN has a higher PA than does the unlabeled acetonitrile (inverse effect). The PA difference of deuterated and unlabeled acetonitrile, however, remains unsettled as the Norrman–McMahon result disagrees with that of Cooks and coworkers [30] and that of Gozzo and Eberlin [31]. Both groups find a normal isotope effect on the proton affinity of acetonitrile. In addition, the latter workers [31] do observe an inverse effect for pyridine. On the basis of these reported results, one would expect that the nature of the secondary isotope effect to be related to structure. Gronert [28] and later Gozzo and Eberlin [31] more reasonably suggest, from results of molecular orbital calculations, that the trends are consistent with differences in zero-point energies, but no one has considered the effect of thermal-energy corrections on these phenomena. Clearly more work is needed to characterize more completely the secondary isotope effects on GB and PA. The kinetic method is the appropriate method for these endeavors.

Acknowledgements

This research project was supported by the NCRR Mass Spectrometry Research Resource at Washington University (NIH Grant No. P41RR00954). The authors wish to thank the Director of the IICT, Hyderabad, for providing facilities. An Encouragement Fellowship from CSIR (to S.P.M.) and UGC (to P.K.), New Delhi, is gratefully acknowledged.

References

[1] J.S. Splitter, F. Turecek, Application of Mass Spectrometry to Organic Stereochemistry, VCH, New York, 1993.
[2] S.P. Gygi, B. Rist, S.A. Gerber, F. Turecek, M.H. Gelb, A. Reudi, Nat. Biotechnol. 17 (1999) 994.
[3] M. Sawada, Mass Spectrom. Rev. 16 (1997) 73 (and references therein).
[4] P. Krishna, S. Prabhakar, M. Manoharan, E.D. Jemmis, M. Vairamani, J. Chem. Soc. Chem. Commun. 13 (1999) 1215.
[5] G. Hanel, B. Gstir, T. Fiegele, F. Hagelberg, K. Becker, P. Scheier, A. Snegursky, T.D. Märk, J. Chem. Phys. 116 (2002) 2456.
[6] D. Schroeder, R. Wesendrup, R.H. Hertwig, T.K. Dargel, H. Grauel, W. Koch, B.R. Bender, H. Schwarz, Organometallics 19 (2000) 2608.
[7] E.P. Kyba, J.M. Timko, L.J. Kaplan, F. de Jong, G.W. Gokel, D.J. Cram, J. Am. Chem. Soc. 100 (1978) 4555.
[8] (a) B.J. Deppmeier, A.J. Driessen, T.S. Hehre, W.J. Hehre, J.A. Johnson, P.E. Klunzinger, J.M. Leonard, I.N. Pham, W.J. Pietro, Jianguo Yu, Spartan 02, Wavefunction, Inc., Irvine, CA;
(b) J. Kong, C.A. White, A.I. Krylov, C.D. Sherrill, R.D. Adamson, T.R. Furlani, M.S. Lee, A.M. Lee, S.R. Gwaltney, T.R. Adams, C. Ochsenfeld, A.T.B. Gilbert, G.S. Kedziora, V.A. Rassolov, D.R. Maurice, N. Nair, Y. Shao, N.A. Besley, P.E. Maslen, J.P. Dombroski, H. Dachsel, W.M. Zhang, P.P. Korambath, J. Baker, E.F.C. Byrd, T. Van Voorhis, M. Oumi, S. Hirata, C.P. Hsu, N. Ishikawa, J. Florian, A. Warshel, B.G. Johnson, P.M.W. Gill, M. Head-Gordon, J.A. Pople, J. Comput. Chem. 21 (2000) 1532;
(c) W.J. Hehre, A Guide to Molecular Mechanics and Quantum Chemical Calculations, Wavefunction, Irvine, CA, 2001.
[9] (a) J.J.P. Stewart, J Comp. Chem. 10 (1989) 209;
(b) J.J.P. Stewart, J. Comp. Chem. 10 (1989) 221.
[10] (a) M.J. Frisch, G.W. Trucks, H.B. Schlegel, G.E. Scuseria, M.A. Robb, J.R. Cheeseman, V.G. Zakrzewski, J.A. Montgomery, Jr., R.E. Stratmann, J.C. Burant, S. Dapprich, J.M. Millam, A.D. Daniels, K.N. Kudin, M.C. Strain, O. Farkas, J. Tomasi, V. Barone, M. Cossi, R. Cammi, B. Mennucci, C. Pomelli, C. Adamo, S. Clifford, J. Ochterski, G.A. Petersson, P.Y. Ayala, Q. Cui, K. Morokuma, D.K. Malick, A.D. Rabuck, K. Raghavachari, J.B. Foresman, J. Cioslowski, J.V. Ortiz, A.G. Baboul, B.B. Stefanov, G. Liu, A. Liashenko, P. Piskorz, I. Komaromi, R. Gomperts, R.L. Martin, D.J. Fox, T. Keith, M.A. Al-Laham, C.Y. Peng, A. Nanayakkara, C. Gonzalez, M. Challacombe, P.M.W. Gill, B. Johnson, W. Chen, M.W. Wong, J.L. Andres, C. Gonzalez, M. Head-Gordon, E.S. Replogle, and J.A. Pople, Gaussian 98, Rev. A.7, Gaussian, Inc., Pittsburgh, PA (1998);
(b) M.J. Frisch, A. Frisch, Gaussian 98, User's Reference, Gaussian, Inc., Pittsburgh, PA, 1999.
[11] A. Nicolaides, D.M. Smith, F. Jensen, L.J. Radom, J. Am. Chem. Soc. 119 (1997) 8083.
[12] A.P. Scott, L. Radom, J. Phys. Chem. 100 (1996) 16502.
[13] R.G. Cooks, J.S. Pratrick, T. Kotiaho, S. McLuckey, Mass Spectrom. Rev. 13 (1994) 287.
[14] R.G. Cooks, P.S.H. Wong, Acc. Chem. Res. 31 (1998) 379.
[15] W. Shen, P.S.H. Wong, R.G. Cooks, Rapid Commun. Mass Spectrom. 11 (1997) 71.
[16] X. Cheng, Z. Wu, C. Fenselau, J. Am. Chem. Soc. 115 (1993) 4844.
[17] Z. Wu, C. Fenselau, Rapid Commun. Mass Spectrom. 8 (1994) 777.
[18] P.B. Armentrout, J. Mass Spectrom. 34 (1999) 74.
[19] L. Drahos, K. Vekey, J. Mass Spectrom. 34 (1999) 79.
[20] R.G. Cooks, J.T. Koskinen, P.D. Thomas, J. Mass Spectrom. 34 (1999) 85.
[21] A.G. Harrison, Mass Spectrom. Rev. 16 (1997) 201.
[22] E.P.L. Hunter, S.G. Lias, J. Phys. Chem. Ref. Data 27 (1998) 413.
[23] G. Bojensen, T. Breindahl, J. Chem. Soc. Perkin Trans. 2 (1994) 1029.
[24] B.D. Nourse, R.G. Cooks, Int. J. Mass Spectrom. Ion Process. 106 (1991) 249.

[25] T.T. Dang, E.L. Motell, M.J. Travers, E.P. Clifford, G.B. Ellison, C.H. DePuy, V.M. Bierbaum, Int. J. Mass Spectrom. Ion Process. 123 (1993) 171.
[26] J.K. Kim, S.H. Sohn, K.S. Yang, S.W. Hong, J. Photosci. 6 (1999) 157.
[27] F. Jensen, J. Am. Chem. Soc. 114 (1992) 9533.
[28] S. Gronert, T.D. Williams, Org. Mass Spectrom. 29 (1994) 151.
[29] K. Norrman, T.B. McMahon, Int. J. Mass Spectrom. 182/183 (1999) 381.
[30] T.I. Williams, J.W. Denault, R.G. Cooks, Int. J. Mass Spectrom. 210/211 (2001) 133.
[31] F.C. Gozzo, M.N. Eberlin, J. Mass Spectrom. 36 (2001) 1140.